# Experimental study of flat plate solar collector performance with twisted heat pipe



IOP Conf. Series: Materials Science and Engineering **518** (2019) 032035 doi:10.1088/1757-899X/518/3/032035

# Experimental study of flat plate solar collector performance with twisted heat pipe

**Basil N. Merzha[1*], Majid H. Majeed[2], Fouad A. Saleh[3]**
[1]Al-Furat Al-Awsat Technical University, Najaf, Iraq
[2]Middle Technical University, Baghdad, Iraq
[3]Mustansiriyah University, Baghdad, Iraq

**Abstract.** In this work, a system of heat pipe is implemented to improve the performance of flat plate solar collector. The experiment rig consists of sun light simulator, flat plate, heat pipe (wickless), heat exchanger, and measurement instruments. The model is represented by twisting portion of the evaporator section and also inclined by an angle of 30$^o$ with a constant total length of 1140 mm. In this model the evaporator, adiabatic and condenser lengths are 780mm, 140mm and 230mm respectively. The omitted energies from sun light simulator are 200, 400, 600, 800 and 1000 W/m$^2$ which is close to the normal solar energy in Iraq. The working fluid for all models is water with fill charge ratio of 30% and the efficiency of the solar collector is investigated with three values of condenser inlet water temperatures, namely (12, 16 and 20$^o$ C). The experimental result showed an optimum volume flow rate of cooling water in condenser at which the efficiency of collector is a maximum. This optimum agree well with the ASHRA standard volume of flow rate for conventional tasting for flat plate solar collector. When the radiation incident increases the thermal resistance of thermosyphon is decreases, where the heat transfer from the evaporator to condenser increases. The experimental results showed the performance of solar collector with twisted evaporator greater than other types of evaporator as a ratio 13.5 %.

**Keywords:** Thermosyphon, flat plate, solar collector, wickless heat pipe

## 1. Introduction

Solar energy is considered one of the best sources of energy for many advantages. It is a huge source of potential energy, which can be obtained freely. It is also one of the permanent sources of energy which is inexhaustible and reliable because of its permanence and continuity. The fossil energy sources are causing pollution to the environment by the emission of carbon dioxide, as well as the problems of global warming, which is a serious problem now and the near future. Heat pipes which are implemented still in its young stage of development and studies, more and deep investigations are required to integrate heat pipe in solar collector systems in order to improve the heat transport)

The advantages of using the thermosiphon [1] long life because it has no moving parts and does not need the energy to power it in addition to the ability to work in minimum temperature difference. Moreover, it does not require maintenance except cleaning plus the parts are very compact and flexible in size, very simple in design and the heat transfers in one way known (thermal diode), and small area demanded. Some researchers have presented theoretical studies, including Hull, J. R., 1986 [2] was studied the effect of the heat pipe in the solar collector on its efficiency. Others carried out practical and theoretical studies. Bong, et al., 1993 [3] produced a solar collector with thermosyphon and the effect of the condenser temperature on efficiency. Lima and Palanyana, 2000 [4] studied the effect of different surfaces on the performance of the solar complex. While H.M.S.

Hussein, 2002 [5] and Nada et.al., 2004 [6] studied the performance of solar collector at the unstable state, where they studied the effect of natural flow on the performance of the solar collector and discussed the process and theory of the effect of mass flow rate and the effect of the temperature of water entry and that the effect of the number of heat pipes placed in the solar collector have an impact on Performance. Esen M, Esen H, 2005 [7] has built a solar collector with Thermosyphon and studied its effect of changing working fluids.

## 2. Theoretical analysis

The Environmental pollution has become a major burden and a major problem affecting life in general, so solar energy can be used as one of the effective ways to treat this problem as well as the problem of lack of electricity. One solar energy application is the use of flat plate solar collectors to heat of water for different uses. Solar collectors with flat plate were begun spread widely for cheap production costs and also operate without the system of tracking the sun like any other types**[8]**. One application of these collectors is the flat plate solar collectors. The heat pipe is a container closed its ends and filled with a small amount of working fluid and have very low thermal resistance.

The simple flat plate solar collector consists of a flat plate and the heat pipe sit in this plate that sealed and evacuated pipe lined with an annular porous wicking material and a small amount of working fluid in liquid state filled the wick. The vapor of working fluid flow in center core of the pipe. The glass cover placed upon it. Figure 1 shows the principle of possible thermal loss of a typical flat plate collector. The common methods of heat loss are infrared radiation exchanges, convection heat loss and conduction through the insulations.

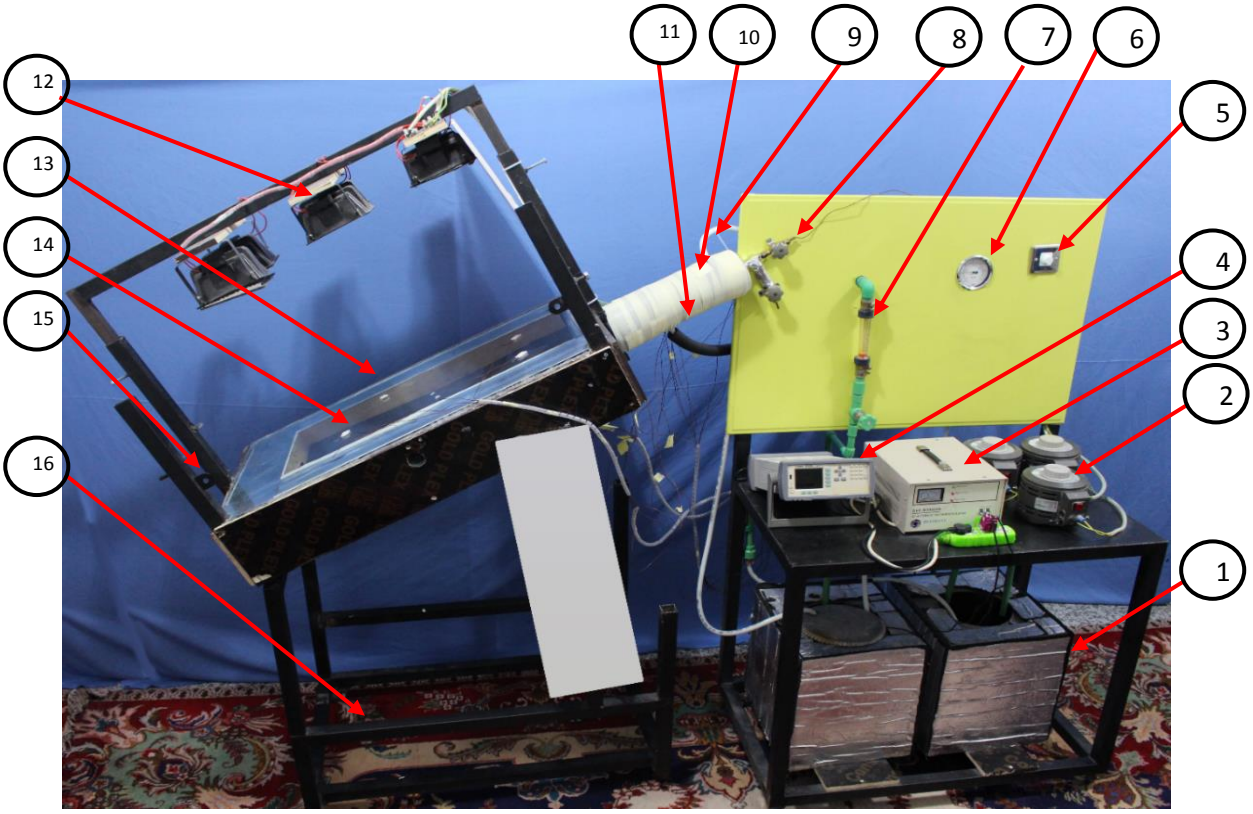


**Figure 1.** Experimental Rig, 1) Water tank, 2) Variable AC Transformer, 3) AC Automatic Voltage Regulator, 4) AT45X data acquisition, 5) Power Switch, 6) pressure gauge, 7) Flow meter, 8) Charging Valve, 9) Outlet water condenser, 10) condenser, 11) Inlet water condenser, 12) Halogen light, 13) glass cover, 14) Flat plate with evaporator, 15) frame, 16) Base of collector.

For glass cover: The balance of energy (W/m$^2$) per a unit area of the collector is denoted as shown in figure 2:

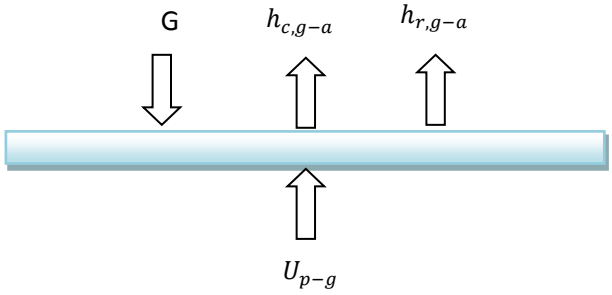


**Figure 2.** Energy balance in the glass of solar collector

$$E_{in\ glass} = E_{out\ glass}$$

$$\rho_g \delta_g C_g \frac{dT_g}{dt} = \alpha_g\, G + U_{p-g}(T_p - T_g) - h_{c,g-a}\,(T_g - T_a) - h_{r,g-a}(T_g - T_a) \text{---------- (1)}$$

For steady state

$$\alpha_g\, G + U_{p-g}(T_p - T_g) - h_{c,g-a}\,(T_g - T_a) - h_{r,g-a}(T_g - T_a) = 0 \text{ ---------- (2)}$$

From Duffie and Bekeman

$$h_{r,g-a} = \frac{\sigma\, \varepsilon_g (T_g + T_s)(T_g^2 + T_a^2)(T_g - T_s)}{(T_g - T_a)} \text{ -------- (3)} \quad \text{When } T_s = T_a$$

$$\therefore h_{r,g-a} = \sigma\, \varepsilon_g (T_g + T_a)(T_g^2 + T_a^2) \text{ ---------- (4)}$$

The external radiation heat transfer coefficient between the glass and ambient depended on wind velocity ($v_w$) can calculated from **[9]** For $0 \le v_w < 10$**:**

$$h_{c,g-a} = 5.7 + 3.8\, v_{wi} \text{ ---------- (5)}$$

$$U_{p-g} = \frac{1}{\frac{1}{h_{r,p-g}} + \frac{1}{h_{c,p-g}}} \text{ ---------- (6)}$$

The radiation coefficient from the plate to glass is:

$$h_{r,p-g} = \frac{\sigma\,(T_p + T_g)(T_p^2 + T_g^2)}{\frac{1}{\varepsilon_p} + \frac{1}{\varepsilon_g} - 1} \text{ ---------- (7)}$$

Hollands et al., 1976 [10] give the equation for Nusselt number for tilt angle from 0$^o$ to 75$^o$.

$$Nu_{p-g} = 1 + 1.44\left[1 - \frac{1708(\sin 1.8\theta)^{1.6}}{Ra\cos\theta}\right]\left[1 - \frac{1708}{Ra\cos\theta}\right] + \left[\left(\frac{Ra\cos\theta}{5830}\right)^{1/3} - 1\right] \text{ ---------- (8)}$$

$$Ra_{p-g} = \frac{g\,\beta\,(T_p - T_g)\,x^3}{v\,\alpha} \text{ ---------- (9)}$$

$$h_{c,p-g} = \frac{Nu_{p-g}\,k}{x} \text{ ---------- (10)}$$

Where:
$x$: Plate spacing.
For flat plate: The balance of energy (W/m$^2$) per unit area of the collector is denoted as:

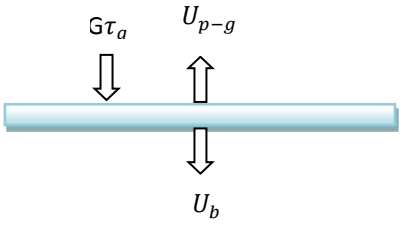


**Figure 3.** Energy balance in the flat plate of solar collector

$$E_{in\ flat\ plate} = E_{out\ flat\ plate}$$

$$\rho_p \delta_p C_p \frac{dT_p}{dt} = \alpha_p \tau_g G + k_p \delta_p \left(\frac{\partial^2 T_p}{\partial x^2}\right) - U_{p-g}(T_p - T_g) - U_b (T_p - T_a) \text{ ---------- (11)}$$

For steady state

$$\alpha_p \tau_g G + k_p \delta_p \left(\frac{\partial^2 T_p}{\partial x^2}\right) - U_{p-g}(T_p - T_g) - U_b (T_p - T_a) = 0 \text{ ---------- (12)}$$

From Duffie and Beckman can be calculated the bottom heat transfer coefficient:

$$U_b = \frac{K_{in}}{\delta_{in}} \text{ ---------- (13)}$$

From boundary condition as shown in figure 4 can be write:

$$\frac{dT_p}{dX} = 0 \ when\ x = 0$$

$$T_p = T_e \quad when\ x = \frac{w}{2}$$

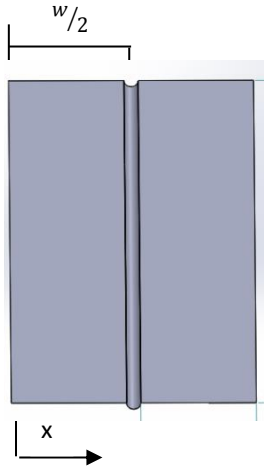


**Figure 4.** The flat plate

For evaporator section: The balance of energy (W/m) for the of the thermosyphon is denoted as:

$$\rho_e A_e C_e \frac{dT_e}{dt} = [\tau_g \alpha_p]_e G \frac{d_o}{2} + k_p \delta_p \frac{\partial T_p}{\partial x} - \frac{\pi d_o}{2} U_{eg}(T_e - T_g) - \pi d_{ei} h_{ei}(T_e - T_s) \text{ ------ (14)}$$

To find Evaporator heat-transfer coefficient inside the evaporator, Shiraishi et al. **[11]** are evaluated:

$$h_{ei} = \frac{4}{3}\left[\frac{\rho_{wa}^2 k_{wa}^3 g\, h_{fg}}{4\mu_{wa}(T_e - T_s)L_e}\right]^{1/4} \text{ ---------- (15)}$$

$$U_{eg} = \frac{1}{\frac{1}{h_{c,e-g}} + \frac{1}{h_{r,e-g}}} \text{ ---------- (16)}$$

$$h_{c,e-g} = \frac{Nu_{e-g}\, k}{L} \text{ ---------- (17)}$$

$$Nu_{e-g} = 1 + 1.44\left[1 - \frac{1708(\sin 1.8\theta)^{1.6}}{Ra\cos\theta}\right]\left[1 - \frac{1708}{Ra\cos\theta}\right] + \left[\left(\frac{Ra\cos\theta}{5830}\right)^{1/3} - 1\right] \text{---------- (18)}$$

$$Ra_{e-g} = \frac{g\,\beta\,(T_e - T_g)\;x^3}{v\,\alpha} \text{---------- (19)}$$

$$h_{r,e-g} = \frac{\sigma\,(T_e + T_g)(T_e^2 + T_g^2)}{\frac{1}{\varepsilon_e} + \frac{1}{\varepsilon_g} - 1} \text{---------- (20)}$$

The energy balance (w) for working fluid (water) will be saturated liquid because the density for vapor phase compared to liquid phase is small.

$$\frac{\pi d_i^2}{4}\rho_l \varphi L_t C_l \frac{dT_s}{dt} = \pi d_i L_e h_e (T_e - T_s) - \pi d_i L_c h_c (T_s - T_c) \text{---------- (21)}$$

For steady state

$$\pi d_i L_e h_e (T_e - T_s) = \pi d_i L_c h_c (T_s - T_c) \text{--- (22)}$$

In condenser section of the thermosyphon in flat plate solar collector, the heat-transfer coefficient of condensation film ($h_c$) (W/m$^2$ K) may be calculated by the relation concluded by **[12]** as follows:

$$h_c = [0.997 - 0.334(cos\theta)^{0.108}]\left[\frac{k_l^3 \rho_l^2 g h_{fg}}{\mu_l L_c (T_s - T_c)}\right]^{0.25}\left[\frac{L_c}{d_i}\right]^{[0.254(cos\theta)^{0.385}]} \text{----------}$$

(23)

For condenser section: The balance of energy (W/m) of the thermosyphon is represented as:

$$\rho_c A_c C_c \frac{dT_c}{dt} = k_c A_c \frac{\partial^2 T_c}{\partial y^2} + \pi\, d_i h_c (T_s - T_c) - \pi\, d_o h_i (T_c - T_w) \text{---------- (24)}$$

The heat transfer coefficient for convective film ($h_o$) of the water flow rate in the cross direction on the condenser sections of the thermosyphon inside a condenser can be calculate from correlations **[13]**

$$h_o = \frac{Nu\,K}{d_o} \text{---------- (25)}$$

$$Nu = C\,Re^m Pr^{\frac{1}{3}}$$

## 3. Experimental work

A 6 halogen projectors 500-watt have been installed on two tracks. Each track has three units. The group has been tested for one and a half meters, one meter and 50 cm. Radiation was tested at nine different points and showed that the best homogeneity of the radiation is at a height of 50 cm.as shown in figure 5.

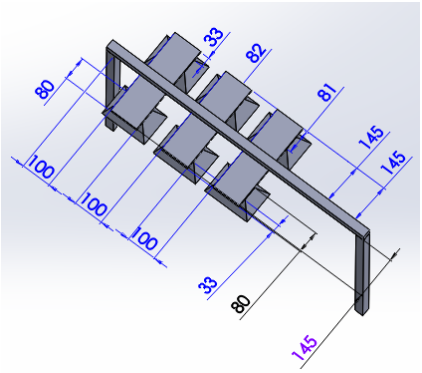


**Figure 5.** The halogen simulator

In the manufacturing flat plate, it was choosing the aluminum material, the thickness is 0.4 mm and width of 32 cm and 78 cm length. This flat plate contain groove to sit the evaporator of heat pipe and put it in wooden structure, the wood thickness of three sides 1 cm. The wooden structure was isolated by placing a thermal insulation around it. The flat plate was painted by black color to increase the absorption.

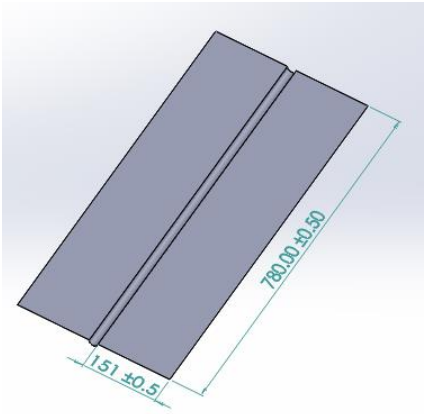


**Figure 6.** The evaporator groove in flat plate

The structure of solar collector is made from the iron, the cross sectional area 2 $in^2$ square shape, the solar collector dimensions is (1 × 0.6) meters, it can be moved about the axis, and fixes at 30° angle [14]. This box contains the isolation that thickness 0.09 m under the flat plate, under the isolation putting the wood that thickness 0.01m. The solar collector has a square base at a height of 0.80 m.

The main components of a heat pipe are the working fluid, the container and the capillary structure or without wick is called thermosyphon [15]. The three types of heat pipe were fabricated which is 1150 mm long.

The condenser is made from PVC (Polyvinyl chloride) because it's softer and more flexible in construction. It is 230 mm long and 69.8mm in diameter and surrounds the copper tube. The condenser has two holes for entering and exiting the water, the ends of the condenser are sealed by sealing between the end of the condenser and the tube to prevent exiting the water out of the condenser. The adiabatic and condenser section are covered with Glass wool insulation to be 75 mm.

The evaporator part has been fixed with the flat plate inside the cavity width of cavity as far as the outlet diameter of the heat pipe and the half the area of evaporator is exposed to radiation. In present work, were fabricated partially helical twisted for thermosiphon. The evaporator of helical twisted consist of two twisted pipe part as long 27 cm between them smooth part as long 10cm, in the each of end evaporator two smooth part 8cmand 6cm as shown in figure 7.

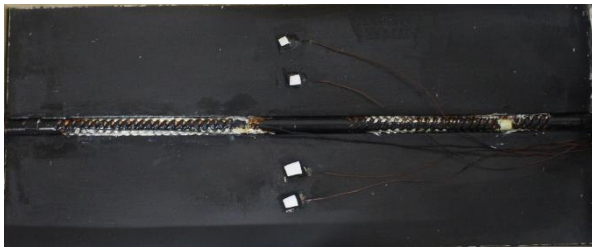

**Figure 7.** The partially twisted evaporator of wickless heat pipe

The selection of the working fluid mainly operates in room temperature. The working fluid used in present work is the water, the temperature operating range from (200) to (500)K **[16]**. Because the water has good wetting characteristics with the wick and container wall material. Also, it has good latent heat and good thermal conductivity.

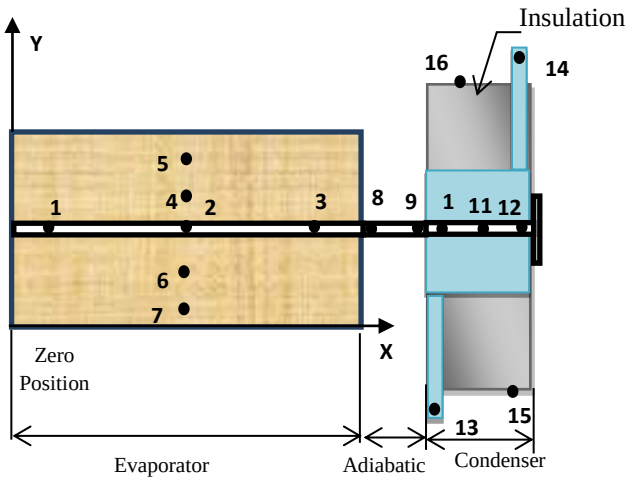


**Figure 8.** The locations of thermocouples

**Table 1.** Specifications of Experimental wickless Heat Pipes.

| Name | Symbol (Unit) | values |
|---|---|---|
| Width of flat plate | ($w_p$)mm | 230 |
| Long of flat plate | ($L_p$)mm | 780 |
| Air gap | ($x_a$)mm | 45 |
| Container outer diameter | ($D_o$) mm | 19 |
| Working length | (L) mm | 1150 |
| length of Evaporator | ($L_e$) mm | 780 |
| length of Adiabatic | ($L_a$) mm | 130 |
| length of Condenser | ($L_c$) mm | 230 |
| Vapor radius | ($r_v$) mm | 12.4 |
| Working fluid | water | - |
| State | degree | 30 |

## 4. Results and discussion

The effect of energy incident variation on thermosyphon behavior was represented in Figure 9, also the axial wall temperature distribution for five different values of energy incident for volume flow rate 20l/h was represented. Whereas, with increasing of the energy incident the working fluid volume flow rate increases so that the saturation pressure increases, all this lead to increase the wall temperature along the thermosyphon.

Figure 10 shows the effect of variation of volume flow rate of water on temperature distribution, while the other parameters are kept constants. As shown from this figure it can be notice that the wall temperature only slightly changed with volume flow rate.

To investigate the thermal behavior of the thermosyphon for different inlet water temperatures, all experiments are accomplished for three inlet water cooling temperatures at the thermosyphon condenser section. Figure 11 shows the influence of sink temperature ($T_{win}$) on axial wall temperature distribution of the thermosyphon for constant energy radiation incident. It can be noticed that the wall temperature increases as the sink temperature increases. This is due to the increasing of the working fluid density which leads to increase the operation temperature.

Figure 12 shows the variation of the thermal resistance of the heat pipe for constant volume flow rate and three inlet water temperature 12ºC, 16ºC and 20ºC and various energy radiation incident. From the figure, it is clear that the thermal resistance of heat pipe is relatively high at low heat input and decreases when the heat input increases.

Figure 13 shows the relationship between the efficiency of the solar collector with the variable $[(T_p-T_a)/G]$. and is a linear relationship were plotted with a curve fitting technique. The intersection of the curve with the y-axis is represented $((F_R(\tau\alpha))_e)$ and the intersection the curve with x-axis represented the slope which explain $(F_R U_L)$ which refers to the quantity of energy have been losses from the collector. Figure 13 and Table (2) show that the efficiency of the solar collector increases with the increase of the water flow rate of the condenser from (10-20 l/h) and then decrease by increasing the flow rate to reach (80 l/h).

**Table 2.**

| $\dot{V}l/h$ | $(F_R(\tau\alpha))_e$ | $F_R U_L$ | G(w/m$^2$) |
|---|---|---|---|
| 10 | 0.3962 | 0.669 | 200 |
| 20 | 0.7157 | 1.52 | 200 |
| 40 | 0.6958 | 2.039 | 200 |
| 60 | 0.6926 | 3.257 | 200 |
| 80 | 0.52 | 2.06 | 200 |
| 10 | 0.5359 | 5.624 | 400 |
| 20 | 0.7818 | 5.838 | 400 |
| 40 | 0.65 | 1.727 | 400 |
| 60 | 0.7038 | 7.416 | 400 |
| 80 | 0.5336 | 2.31 | 400 |
| 10 | 0.5139 | 10.57 | 600 |
| 20 | 0.7727 | 12.226 | 600 |
| 40 | 0.7084 | 6.44 | 600 |
| 60 | 0.7026 | 10.41 | 600 |
| 80 | 0.6869 | 8.5964 | 600 |
| 10 | 0.3496 | 1.9 | 800 |
| 20 | 0.8777 | 17.844 | 800 |
| 40 | 0.8356 | 10.646 | 800 |
| 60 | 0.7752 | 12.18 | 800 |
| 80 | 0.7246 | 13.169 | 800 |
| 10 | 0.4212 | 0.1377 | 1000 |
| 20 | 0.8575 | 16.543 | 1000 |
| 40 | 0.8381 | 12.676 | 1000 |
| 60 | 0.8323 | 15.594 | 1000 |
| 80 | 0.6616 | 5.1373 | 1000 |

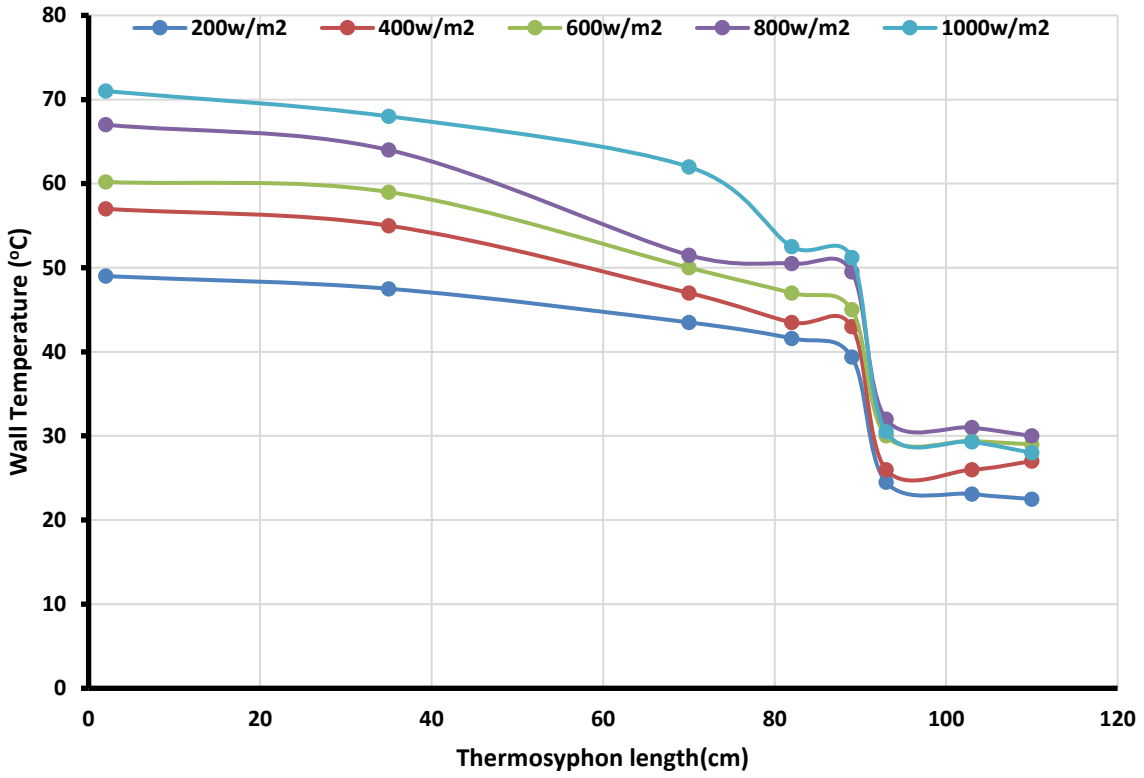


**Figure 9.** Effect enrgy radaition on the wall temperature with flow rate 20L/h at inlet water temperature is 16 for Twestied evaporator

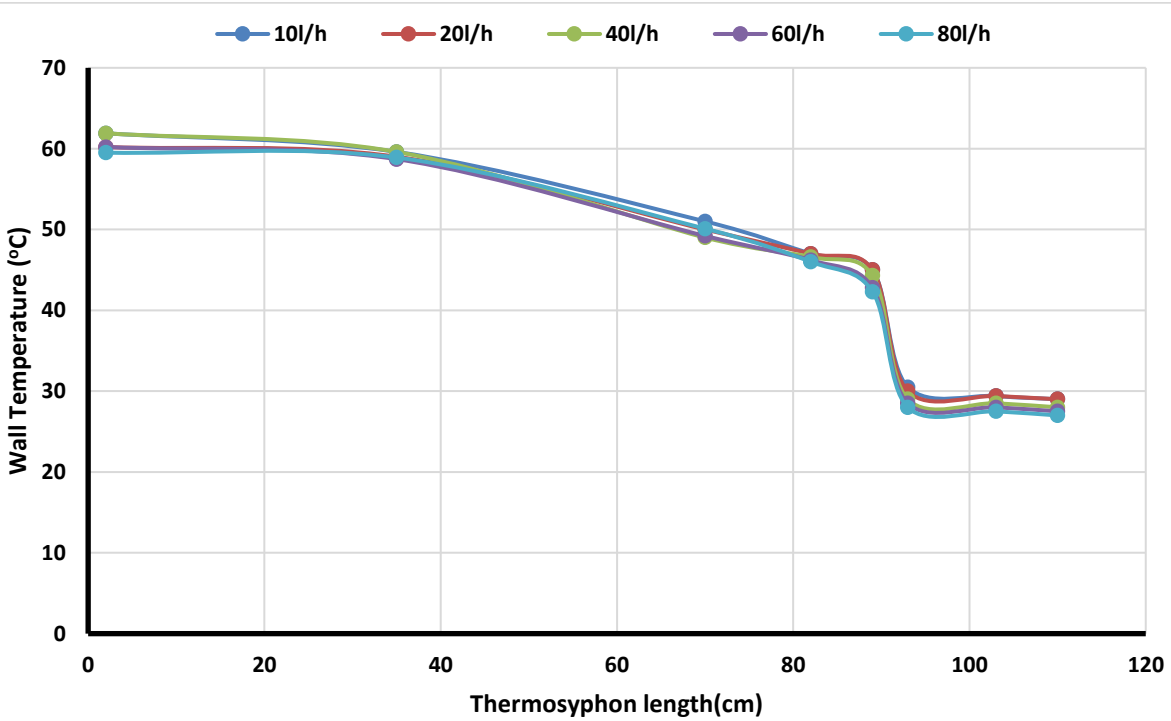


**Figure 10.** Effect the volume flow rate on the thermosyphon wall temperature distribution at radiation energy 600w/m$^2$ and inlet water temperaure 16$^o$C for twisted evaporator

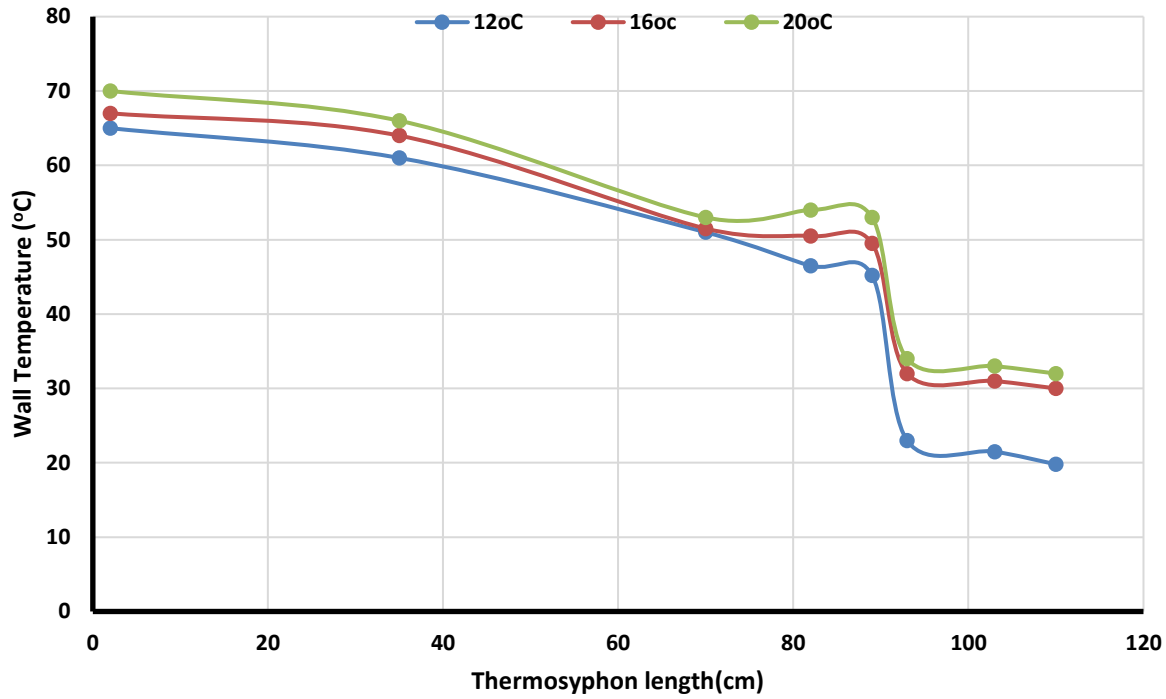


**Figure 11.** Effect the inlet water temperature on the thermosyphon wall temperature distribution at radiation energy 800 w/m$^2$ and flow rate 20l/h for twisted evaporator

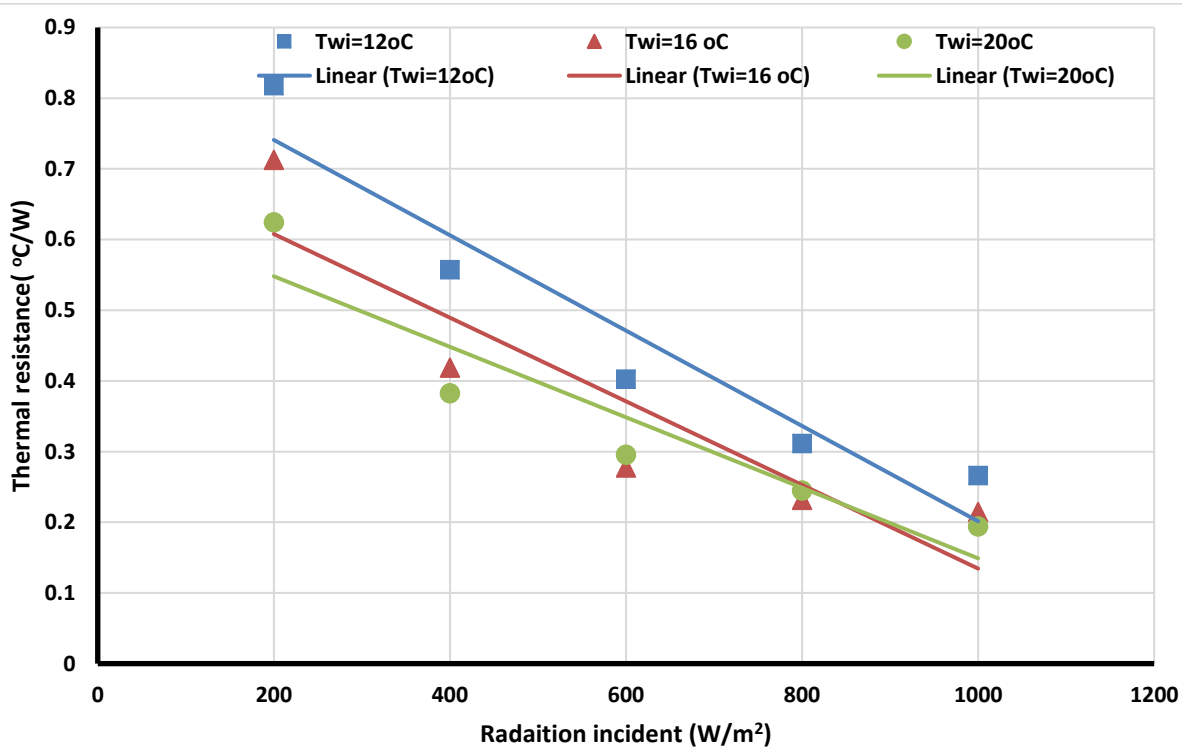


**Figure 12.** Effect the radaition incident on the thetmal resistance for flow rate 10/lh for twisted evaporator

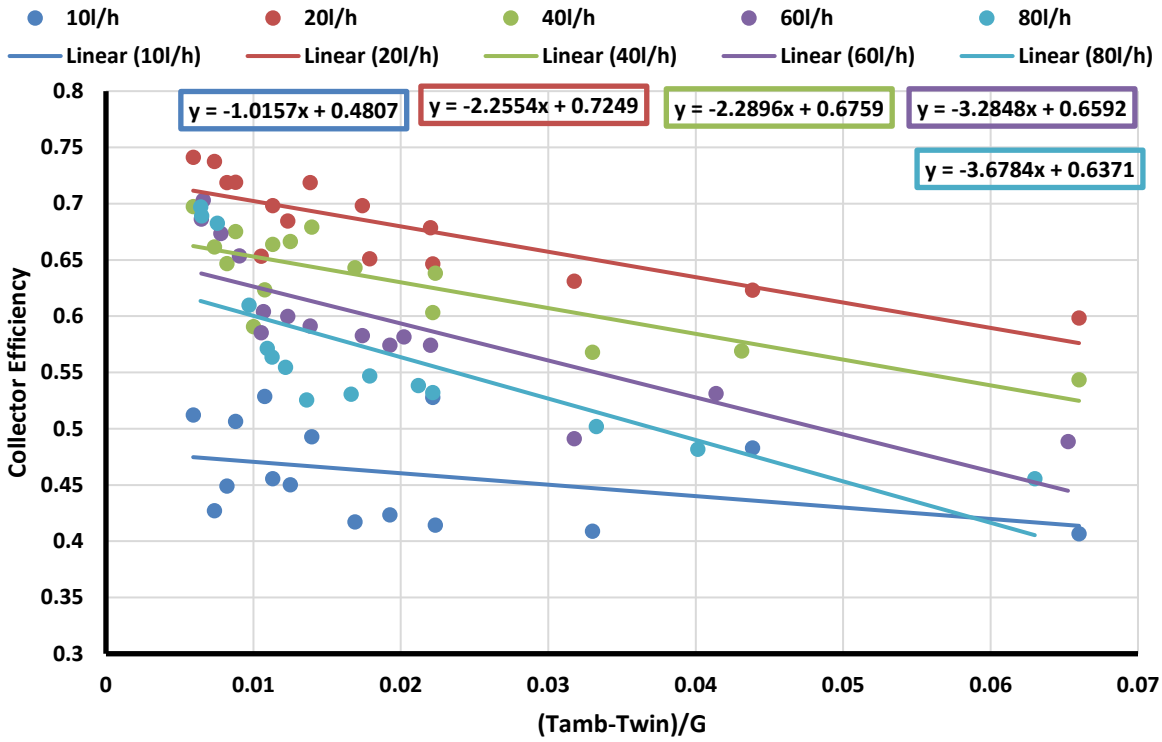


**Figure13.** The effect of [($T_{amb}$-$T_{win}$)/G ]on the collector efficiency for differant flow rate for twisted evaporator

## 5. Conclusion

The flat plate solar collector with thermosyphon was studied experimentally. It is hoped that the information included in present study will help engineers to become more familiar with the various options available in the use of heat pipe in solar collector by for enhancement the efficiency of collector by use twisted shapes of evaporator. From the experimental woke the flowing can be concluded:

1- The experimental testes were demonstrated the pest volume flow rate of cooling water in condenser when$\dot{m}_{win} = 0.02\ A$ at which the efficiency of collector is a greatest. This flow rate equal to 4.35 l/h in each model for numerical and equal to 20l/h for experimental because different area. This optimum approves with the ASHRA Standard volume flow rate for exam the conventional solar water collectors.

2- When the radiation incident increases the thermal resistance of thermosyphon is decreases, where the heat transfer from the evaporator to condenser increases.

3- The experimental result showed the performance of solar collector with twisted evaporator shape greater than conventional thermosyphon solar collector as a ratio (13.5) %.

## NOMENCLATURE

A: Cross section Area ($m^2$)
C: Specific heat (kJ/kg)
d: Diameter(m)
G: Intensity radiation ($W/m^2$)
h: Heat transfer coefficient ($W/m^2$. K)
Nu: Nusselt number
Pr: Prandtl Number ( ν/α)
$T_a$: Adiabatic section ($^oC$)

$T_{amb}$: Ambient temperature ($^oC$)
X: Air gap (m)
w: Width(m)
v : Specific volume( $m^3/kg$ )
μ: Dynamic viscosity $N.s/m^2$
ρ : Density ($kg/m^3$ )
σ : Surface tension (N/m)
δ : Thickness (m)
ϵ: Emissivity
α : Absorptance
θ : Tilt angle from horizontal.
$\theta_i$ : incident angle
β : Volumetric coefficient of expansion.
τ : Transmittance.

## References

[1] Zohuri, B., *Heat pipe design and technology*. 2011: Springer.
[2] Hull, J., 1986 Analysis of heat transfer factors for a heat pipe absorber array connected to a common manifold. *Journal of solar energy engineering*, **108**(1): p. 11-16.
[3] Bong, T., K. Ng, and H. Bao, 1993 Thermal performance of a flat-plate heat-pipe collector array. *Solar Energy*, **50**(6): p. 491-498.
[4] Lima, W. and A. Palangana, 2000 Flat plate solar collector with heat pipes and selective surfaces. *Latin American Applied Research*, **30**(3): p. 249-251.
[5] Hussein, H., 2002 Transient investigation of a two phase closed thermosyphon flat plate solar water heater. *Energy Conversion and Management*, **43**(18): p. 2479-2492.
[6] Nada, S., H. El-Ghetany, and H. Hussein, 2004 Performance of a two-phase closed thermo syphon solar collector with a shell and tube heat exchanger. *Applied Thermal Engineering*, **24**(13): p. 1959-1968.
[7] Esen, M. and H. Esen, 2005 Experimental investigation of a two-phase closed thermosyphon solar water heater. *Solar Energy*, **79**(5): p. 459-468.
[8] Kalogirou, S.A., 2004 Solar thermal collectors and applications. *Progress in energy and combustion science*, **30**(3): p. 231-295.
[9] Duffie, J.A., Beckman, W. A., *Solar Engineering of Thermal Processes, ed. s. edition*. 1991: John Wiley & Sons, Inc.
[10] Hollands, K., et al., 1976 Free convective heat transfer across inclined air layers. *Journal of Heat Transfer*, **98**(2): p. 189-193.
[11] Shiraishi, M., K. Kikuchi, and T. Yamanishi, 1982 Investigation of heat transfer characteristics of a two-phase closed thermosyphon, in Advances in Heat Pipe Technology. *Elsevier*. p. 95-104.
[12] Hussein, H., 2007 Theoretical and experimental investigation of wickless heat pipes flat plate solar collector with cross flow heat exchanger. *Energy Conversion and Management*, **48**(4): p. 1266-1272.
[13] Janna, W.S., *Engineering heat transfer*. 2011: CRC Press.
[14] Imad Jawad Khadim, E.J.M., Ali Hussian Ubaid, 2014 Determining Tilt Angle for Fixed Solar Panel Tosites of Iraq's Provinces by Using the Programs on NASA and Google Earth Websites. *Eng. &Tech.Journal*, **32**: p. 3.
[15] Chi, S., 1976 Heat pipe theory and practice. *Washington, DC, Hemisphere Publishing Corp.; New York, McGraw-Hill Book Co.*, **256**, p., 1976.
[16] Yang, X., Y. Yan, and D. Mullen, 2012 Recent developments of lightweight, high performance heat pipes. *Applied Thermal Engineering*, **33**: p. 1-14.